10. Yu. N. Rabotnov, Elements of the Hereditary Mechanics of Solids [in Russian], Nauka, Moscow (1977).
11. T. D. Shermergor, "Effective rheological characteristics of laminar materials," Izv. Akad. Nauk SSSR, Mekh. Tverd. Tela, No. 1 (1971).
12. S. I. Meshkov, G. N. Pachevskaya, and V. S. Postnikov, "Behavior of materials under high intensity dissipative processes," Fiz. Khim. Obrab. Materialov, No. 2 (1967).
13. C. Ziener, "Elasticity and inelasticity of metals," in: Elasticity and Inelasticity of Metals [Russian translation], IL, Moscow (1954).
14. S. I. Meshkov, "On the description of internal friction in hereditary elasticity theory by using kernels possessing a weak singularity," Zh. Prikl. Mekh. Tekh. Fiz., No. 4 (1967).
15. E. S. Solodysheva, N. I. Korshuk, et al., "On the influence of the cooling rate on certain physicomechanical characteristics of stiff cross-linked polymers," Composite Polymer Materials [in Russian], No. 6, Kiev (1980).
16. A. M. Skudra, É. Z. Plume, and G. M. Gunyaev, "Properties of glass-plastics reinforced by high-modulus fibers," Mekh. Polim., No. 1 (1972).
17. S. I. Meshkov, G. N. Pachevskaya, and T. D. Shermergor, "On the description of internal friction by using fractional-exponential kernels," Zh. Prikl. Mekh. Tekh. Fiz., No. 3 (1966).
18. G. M. Gunyaev, A. F. Rumyantsev, et al., "Investigation of dynamic characteristics of composite materials," Mekh. Polim., No. 2 (1974).

DYNAMIC PHOTOELASTIC PROPERTIES OF AN EPOXY RESIN ABOVE THE ELASTIC LIMIT

B. M. Zhiryakov, V. G. Malinin, and V. F. Obesnyuk

UDC 539.30

Epoxy resins are widely used as optically sensitive stress transducers for both static and dynamic loading methods. Their photoelastic properties have been well studied in the range of elastic deformation down to loading times on the order of 10^{-5} sec [1, 2]. However, there is almost no experimental data in the literature for compression above the elastic limit due to the brittle fracture of glassy polymers. In the present study, we were successful in measuring the photoelastic effect in a broader range of pressures by loading the material with compression pulses of about 10^{-7} sec duration.

1. Experimental Unit and Measurement Method. The compression pulses were created by a laser operated in the modulated Q-factor regime. The duration of the laser pulse was 30 nsec at half-height. The output energy was 0.65 J and the diameter of the focal spot was about 1 mm. Focusing was done on a specimen of ED-6, the surface of which was covered by a 50-μm-thick copper foil. A film of distilled water about 1 mm thick was placed on the foil to obtain sufficiently high pressures. The amplitude of the pressure pulses in the polymer here was on the order of 1 GPa, with a duration of about 10^{-7} sec. Figure 1 shows a profile of the pressure pulse (time scale of grid 50 nsec) obtained with a thin (100 μm) quartz transducer. The profile is extended somewhat compared to the radiation pulse, a fact connected with the multiple reflections and interference of the pressure pulse in the foil due to the substantial difference in the acoustic impedances of the copper and epoxy resin.

We used a standard method [1] to observe the dynamic photoelastic effect. We used a variant in which the transmitting radiation passed through a specimen placed between an analyzer

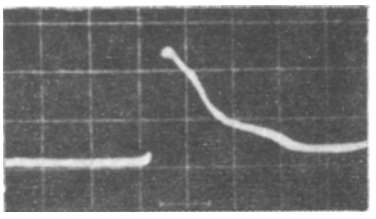

Fig. 1

Moscow. Translated from Zhurnal Prikladnoi Mekhaniki i Tekhnicheskoi Fiziki, No. 6, pp. 145-148, November-December, 1984. Original article submitted September 22, 1983.

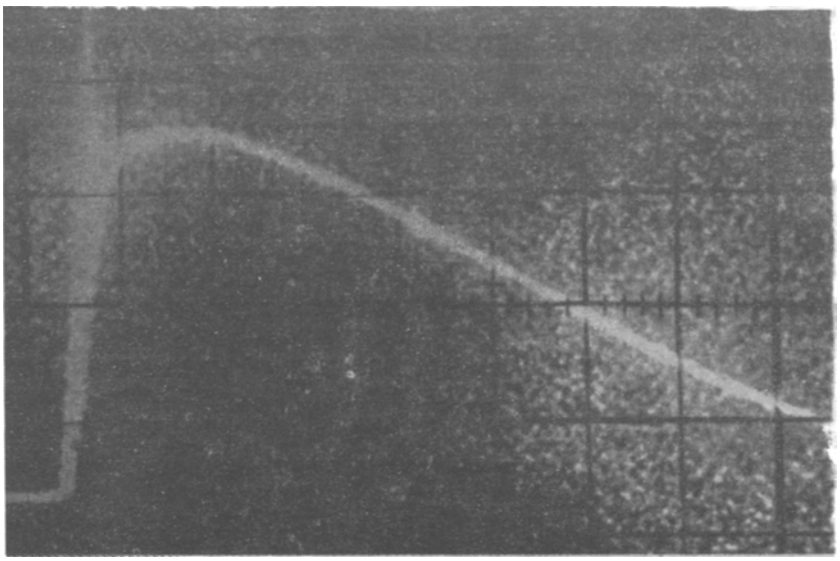

Fig. 2

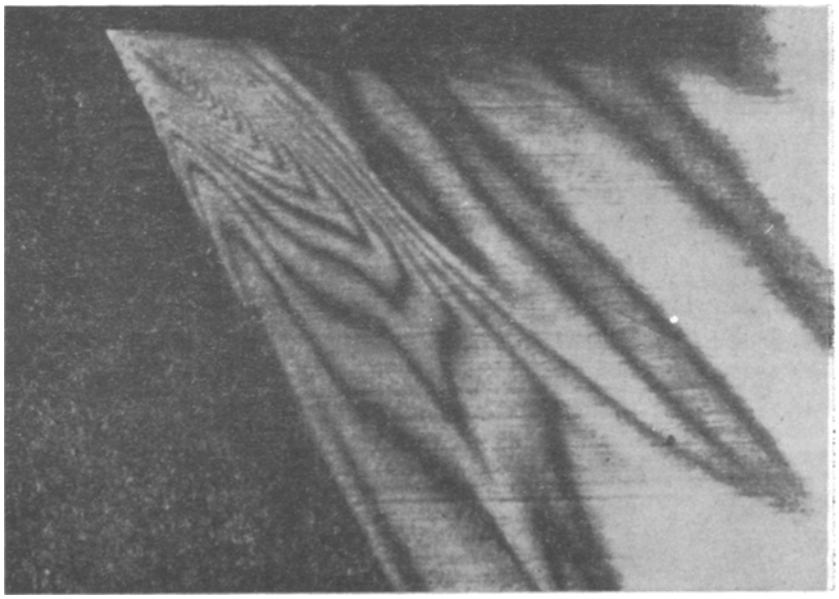

Fig. 3

and polarizer in the crossed position. An image was obtained over time by slit scanning on KN-4 film with an SFR-1M high-speed camera. Another ruby laser (λ = 0.693 μm) was used as an intense monochromatic light source. This layer was synchronized in time with the first laser and the SFR-1M camera. Operation of the transmitting laser in the smooth-pulse regime, with pulses of about 0.8 msec (Fig. 2), ensured the necessary exposure of the film.

Figure 3 shows a typical fringe pattern obtained on an epoxy specimen with a height of 15 mm, width of 30 mm, and transmission thickness of 1.98 mm. Lines (in the coordinates z, t) along which longitudinal and shear waves propagate are clearly visible in the figure. Because the loading was close to concentrated in character, the shear wave is fairly powerful. The line of propagation of the leading edge of the longitudinal compression wave is somewhat curved, the curvature being greater, the closer to the loading surface. The velocity far from this surface approaches the sonic velocity, which for control purposes was also measured (by an independent method). Such behavior of velocity is connected with the nonlinear acoustic properties of the epoxy resin. Its determination makes it possible to use the pattern obtained to calculate the pressure at the wave front by means of the familiar Hugoniot relation [3] $\sigma_{zz} = \rho_0 Du$ and the linear relation between the shock wave velocity and the mass velocity $D = c_0 + Bu$, where c_0 is a constant close to the sonic velocity in epoxy resin; u is the mass velocity; D is the velocity of the shock wave; ρ_0 is the density ahead of the front of the

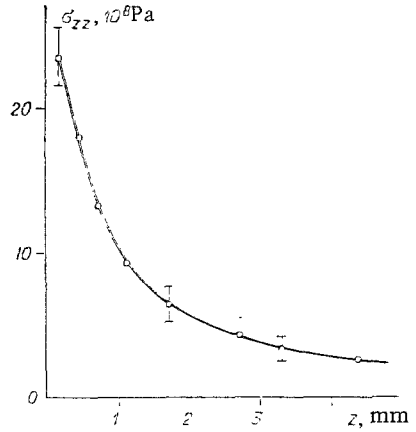

Fig. 4

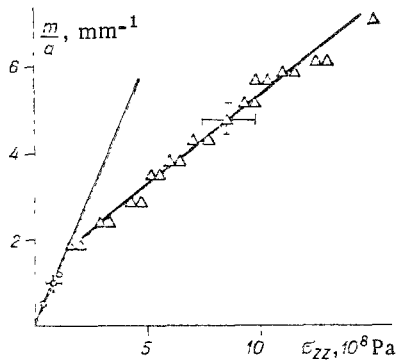

Fig. 5

compression wave; σ_{zz} is the pressure at the wave front; B is a nonlinearity constant (B = 1.52 for epoxy resin [4]).

2. Results of Experiment and Discussion. Figure 4 shows the dependence of the pressure amplitude in the shock wave on the distance traveled for the pattern in Fig. 3. Comparison of the pressures and the observed orders of the interference bands made it possible to construct the relation shown in Fig. 5. The above method did not provide the necessary accuracy at $\sigma_{zz} \leqslant 100$ MPa, so for low pressures we used a somewhat different target design. We placed a polymeric compound with a low compression modulus between the foil and epoxy resin. The velocity of the shock wave was still appreciably greater than the sonic velocity at pressures in the compound of about 100 MPa, which assured the requisite accuracy in the low-pressure range as well. An example of such a pattern is shown in Fig. 6.

It is apparent from Fig. 5 that the empirical relation is approximated by two straight lines. The photoelastic constant, determined as

$$\sigma^{0,1} = d\delta\sigma_{zz}/\delta m, \tag{1}$$

changes appreciably near 150 MPa from 80 kPa·m to 230 kPa·m. In Eq. (1), d is the effective working dimension along the transmission direction; m is the order of the photoelastic band; δ is a small increment.

Both values differ considerably from the static photoelastic constant. We measured the latter by a standard method on a disk and a beam [1] and found it to be $\sigma_0^{0,1} = 24$ kPa·m. In the range up to 150 MPa the static and dynamic constants were compared with allowance for the differences in the uniaxial stress state in the static case and the uniaxial strain state in the dynamic case. In the latter case, with elastic deformation all of the principal stresses are nontrivial [3]:

$$\sigma_{xx} = \sigma_{yy} = [\nu/(1-\nu)]\sigma_{zz}, \tag{2}$$

where ν is the dynamic Poisson ratio. As a result, the optical effect, proportional to the difference between the principal stresses, turns out to be less by a factor of $(1-\nu)/(1-2\nu)$. Then $(1-\nu)/(1-2\nu)\sigma_0^{0,1} \approx 60$ kPa·m, which is fairly close to the experimental value of the dynamic constant for low pressures.

The abrupt change in the optical properties near 150 MPa is naturally connected with the exceeding of the dynamic elastic limit of resin ÉD-6. Given this, then, on the basis of the experiment, it should be pointed out that an increase in the amplitude of σ_{zz} is accompanied by an approximately linear increase in the dynamic limit Y — at least up to $\sigma_{zz} \approx 1.5$ GPa. This occurs because the increase in amplitude is accompanied by an increase in the optical effect which is proportional to the difference in the principal stresses [1]. As in the case of elastic–plastic deformation, according to the von Mises–Tresca criterion $(\sigma_{zz} - \sigma_{xx}) = Y$. Above the elastic limit, we can use Eqs. (2) and Fig. 5 to determine $\delta Y/\delta\sigma_{zz} \approx 0.16$. Such an estimate agrees well with empirically observed increases in the shear elastic limit for other glassy polymers [5] under hydrostatic compression.

However, the plastic strain of the specimens in our experiments was minimal. Observation of once-loaded specimens in the cross polarizers revealed no visible changes, so we could conclude that the residual stresses were no greater than 30 MPa (which corresponds to

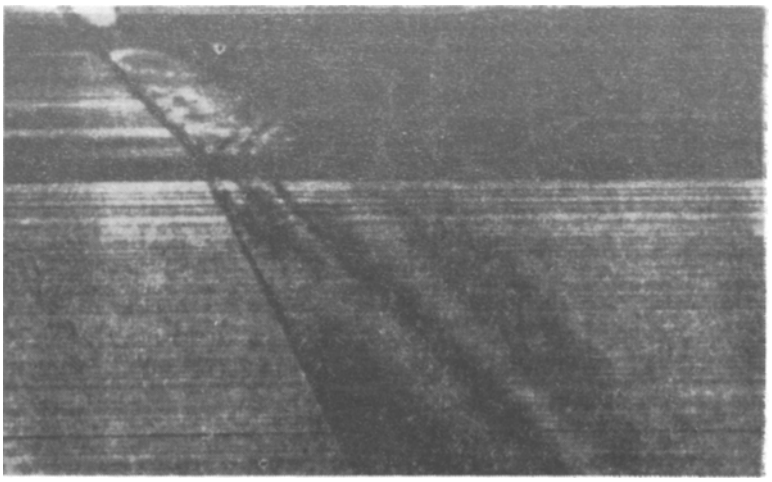

Fig. 6

roughly one-fourth of a band). In the case of loading ten or more times, such changes were cumulative and became noticeable. They were concentrated near the surface in an area of about 1 mm. This behavior argues heavily in favor of the conclusion that, in our experiment, we observed the phenomenon of forced elasticity of epoxy resin in compression above the elastic limit, i.e., almost complete strain reversibility was possible. However, the current view of forced elasticity (see [6]) itself does not describe the behavior of optical properties such as is shown in Fig. 5. For this reason, it is necessary to consider representations on the elastic limit of the resin at pressures in the pulse of about 1 GPa.

Another interesting fact turned out to be the increase in ultimate compressive strength by about one order of magnitude in the event of high-speed deformation (10^6-10^7 sec^{-1}). It is widely believed that for glassy polymers (such as PMMA or polystyrene) an increase in loading rate produces a system of cracks along with the beginning of plastic strain almost immediately after the elastic limit (about 100 MPa) is exceeded, i.e., brittle fracture is observed [1, 7, 8]. This did not occur in our case. It should be noted that control experiments were also conducted with polymethyl methacrylate.

Thus, it was shown experimentally that the results of determination of the photoelastic properties of glassy polymers in elastic-plastic deformation can be used to study the physics of high-rate deformation of the materials, as well as in the application of epoxy resins as pressure transducers.

The photoelastic method is evidently unique, in that it is quite sensitive and makes it possible to obtain directly information on the difference in principal stresses in shock compression. Less refined methods [9] failed to detect the above-noted inflection in the relation.

We quite understand that the findings reported here raise more questions than they answer. We therefore express our gratitude beforehand for any discussions of the results with interested investigators.

LITERATURE CITED

1. A. Ya. Aleksandrov and M. Kh. Akhmetzyanov, Optical-Polarization Methods of the Mechanics of Deformable Bodies [in Russian], Nauka, Moscow (1973).
2. N. A. Strel'chuk and G. L. Khesin (editors), Methods of Photoelasticity, Vols. 1 and 2, Stroiizdat, Moscow (1975).
3. Ya. B. Zel'dovich and Yu. P. Raizer, Physics of Shock Waves and High-Temperature Hydrodynamic Phenomena, Nauka, Moscow (1966).
4. R. MacEwen, S. Marsh, et al., "Equation of state of solids from the results of study of shock waves," in: High-Temperature Shock Effects [Russian translation], Mir, Moscow (1973).
5. A. A. Silano, K. D. Pae, and J. A. Sauer, "Effects of hydrostatic pressure on shear deformation of polymers," J. Appl. Phys., 48, No. 10 (1977).
6. A. A. Askadskii, Deformation of Polymers, Khimiya, Moscow (1973).
7. F. Ramsteiner, "Einfluss von Verarbeitungs und Produktparametern auf die Schlagzähigkeit von Styrol-Polymerisaten," Kunststoffe, 67, No. 9 (1977).

8. G. Kol'skii, Stress Waves in Solids [Russian translation], IL, Moscow (1955).
9. P. F. Chartaguac, "Determination of mean and deviatoric stress in shock loaded solids," J. Appl. Phys., 53, No. 2 (1982).

SELF-SIMILAR SOLUTIONS OF THE DYNAMICS EQUATIONS OF AN IDEAL ELASTIC-PLASTIC BODY UNDER TRESCA PLASTICITY CONDITIONS

G. I. Bykovtsev, A. V. Kolokol'chikov, and P. N. Sygurov

UDC 539.3

Self-similar solutions of the dynamics equations of an ideal elastic-plastic body under Mises plasticity conditions were examined in [1-4], where the solutions of the boundary-value problems were reduced to the solution of two-point problems of nonlinear differential equations with singularities. It is shown below that these equations, under Tresca plasticity conditions, are integrated in quadratures which will permit achievement of significant simplifications.

1. The equations describing the behavior of Prandtl-Reiss bodies have the form

$$e_{ij} = e^p_{ij} + e^e_{ij},\ e_{ij} = \frac{1}{2}(u_{i,j} + u_{j,i}),\ \sigma_{ij} = \lambda e_{kk}\delta_{ij} + 2\mu e^e_{ij}; \tag{1.1}$$

$$\sigma_{ij,j} - \rho\dot{v}_i = 0,\ v_i = \dot{u}_i, \tag{1.2}$$

where u_i is the displacement, and the dot denotes differentiation with respect to time.

Let us consider the plane strain of a medium under Tresk plasticity conditions

$$|\tau_{max}| = k. \tag{1.3}$$

Let σ_{33} be the third principal stress σ_3. We designate the other two such that $\sigma_1 > \sigma_2$. Let us examine possible variations.

A. Let $\sigma_1 > \sigma_3 > \sigma_2$. Then condition (1.3) takes the form

$$\sigma_1 - \sigma_2 = 2k. \tag{1.4}$$

From the associated flow law there follows

$$\dot{e}^p_1 + \dot{e}^p_2 = 0,\ \dot{e}^p_3 = 0,\ \dot{e}^p_1 > 0.$$

Since $e_{33} = 0$, $e^e_{33} = 0$, we have from (1.1)

$$\sigma_3 = \sigma_{33} = (1/2)(\sigma_{11} + \sigma_{22})\lambda(\lambda + \mu)^{-1}.$$

We have for the principal stresses in the Ox_1x_2 plane

$$\sigma_1, \sigma_2 = \sigma \pm \sqrt{(\sigma_{11} - \sigma_{22})^2 + 4\sigma^2_{12}}. \tag{1.5}$$

From the relationships (1.4) and (1.5) there follows

$$(\sigma_{11} - \sigma_{22})^2 + 4\sigma^2_{12} = 4k^2. \tag{1.6}$$

The associated flow law has the form

$$\frac{\sigma_{11} - \sigma_{22}}{2\sigma_{12}} = \frac{\dot{e}^p_{11} - \dot{e}^p_{22}}{2\dot{e}^p_{12}},\ \dot{e}^p_{11} + \dot{e}^p_{22} = 0. \tag{1.7}$$

We satisfy condition (1.6) by setting

$$\sigma_{11} = \sigma + k\cos 2\theta,\ \sigma_{22} = \sigma - k\cos 2\theta,\ \sigma_{12} = k\sin 2\theta, \tag{1.8}$$

where θ is the angle between the first principal direction and the Ox_1 axis. Substituting (1.8) into the relations (1.1), (1.2), and (1.7), we obtain a system of equations to determine σ, θ, v_1, v_2

$$\sigma_{,1} - 2k(\theta_{,1}\sin 2\theta - \theta_{,2}\cos 2\theta) - \rho\dot{v}_1 = 0; \tag{1.9}$$

Kuibyshev. Translated from Zhurnal Prikladnoi Mekhaniki i Tekhnicheskoi Fiziki, No. 6, pp. 148-156, November-December, 1984. Original article submitted November 22, 1983.

0021-8944/84/2506-0941$08.50